KFUPM
Journal of Undergraduate Research International

Diamond Open Access 213

Article Petroleum Engineering

Experimental Investigation of Chemical-Assisted CO_2-EOR: Impacts on Minimum Miscibility Pressure

Abdullah Almahasnah and Arshad Raza*

Cite https://doi.org/10.64589/juri/231586

Submitted: April 26, 2026 Revised: May 17, 2026 Accepted: May 18, 2026

ABSTRACT

CO_2 dissolved in oil reduces its density and viscosity, thereby facilitating oil flow at the miscibility pressure. Therefore, CO_2 flooding is a crucial technique for enhancing oil recovery. The minimum miscibility pressure (MMP) is reached at a relatively high pressure, which might be unfeasible to achieve, either owing to economic limitations, such as pumping power consumption, or because the MMP is higher than the fracture pressure of a reservoir. Therefore, lowering the MMP is crucial. This study investigates the effect of two different chemical additives (i.e., ionic liquids, IL) on MMP reduction. MMP was measured using the Vanishing Interfacial Tension via axisymmetric drop shape analysis. This technique was implemented because it can provide rapid and accurate results, as reported in the literature. The applied chemicals were locally synthesized (not commercially available) at the Center of Integrated Petroleum Research. The first solution, Ionic Liquid 360 (IL360), showed a downward trend in the interfacial tension and a higher estimated MMP. However, the second additive (IL690) resulted in a lower MMP of 3.33% compared to the baseline case.

Keywords: minimum miscibility pressure, vanishing interfacial tension, enhanced oil recovery, CO_2 flooding, chemical EOR

1. INTRODUCTION

Global energy demand is increasing owing to globalization and population growth [1]. Therefore, finding alternative ways to satisfy energy consumption is paramount. Although several strategies can be implemented to meet this demand, countries face challenges in securing the energy they need at an affordable price while remaining environmentally friendly [2]. The integration of renewable sources for co-generation, including solar, wind, and geothermal energy, is an alternative to generate clean energy without increasing the global warming rate [3]. Another approach is to increase oil production, as it accounts for the largest share of energy generation sources, such as in electrical plants [4]. Increasing oil production rates requires either exploring for new fields or developing existing fields through enhanced oil recovery (EOR) methods. Moreover, developing new technologies and methods is vital for extracting hydrocarbons cost-effectively, and consequently, increasing the recovery factor. The EOR approach represents a promising solution for further increasing reservoir oil production beyond conventional methods [5]. The key objective of all the EOR projects is to enhance the overall sweep efficiency of hydrocarbons (see Eq. 1) using injected fluids (water, steam, chemicals, or gas) [6]. To improve sweep efficiency, either the macroscopic sweep (volumetric) efficiency, microscopic displacement efficiency, or both can be improved.

$$E = E_V E_D \tag{1}$$

where E is the overall sweep efficiency; E_V is volumetric, and E_D is microscopic sweep efficiencies, respectively.

Typically, EOR techniques are classified into four categories: Thermal, Chemical, Microbial, and Gas [7]. EOR method was first implemented in the 1920's [8]. Thermal EOR involves injecting steam (hot water) into a reservoir to heat the oil, thereby reducing its viscosity and increasing the capillary number [9]. Another thermal method that utilizes coke-like material as a fuel is in situ combustion (ISC), where an oxidizing gas (air oxygen-rich) is injected into the reservoir that ignites a portion of heavy oil components, i.e., 5–10% of Original-Oil In-Place (OOIP), to transfer thermal energy and, consequently, mobilize heavy crude oil [8]. Thermal EOR techniques are suitable for high-porosity sandstones, where the oil has an American Petroleum Institute (API) gravity of less than 20 (heavy oil) or even less than 10 for extra-heavy crude oil or bitumen [10,11]. In contrast, Chemical EOR techniques encompass the flooding with surfactants, polymers, and alkaline solutions, or surfactants and polymers (SP), alkali and polymers (AP), and alkali/surfactant/polymer (ASP). These methods have demonstrated their efficiency over the past years, as they reduce interfacial tension (IFT), alter wettability, and improve oil mobility [12,13]. The main focus of polymers is mobility control, achieved by increasing the viscosity of the injected fluid (water) to reduce the water relative permeability, thereby lowering the mobility ratio [12].

Water, by itself, seeks the path of least resistance and higher permeability. Therefore, the water bypasses the high-viscosity oil bank without sweeping it, reducing the recovery factor (RF).

Published under an exclusive license by KFUPM

However, the use of polymers reduces the relative permeability of water and increases its viscosity, allowing it to sweep oil in a piston-like manner[14]. In addition, surfactants are used to reduce the IFT at the oil-water interface. Surfactants comprise hydrophilic heads (water-loving) and hydrophobic (oil-loving) tails, which benefit both aqueous and non-aqueous phases owing to their amphiphilic nature[15]. Surfactants are classified based on the hydrophilic group (charge) found on the head. The main categories are anionic, cationic, nonionic, and amphoteric[16]. Usually, after primary and secondary recovery, the remaining residual oil draws a significant portion of the trapped oil in the reservoir, and the residual oil can be freed by increasing the capillary number by reducing the IFT. Therefore, surfactants are injected into the reservoir to accumulate at the liquid-liquid interface, thereby reducing the IFT between oil and water[12]. Furthermore, the alkaline flooding recovery mechanisms are similar to those of surfactants. Alkaline flooding is performed by injecting high-pH water (typically 10–12) prepared with NaOH into the oil reservoir, reacting with organic acids within crude oil, and subsequently forming in-place surface-acting agents[17]. These reactions depend on the acidity of the oil and its composition[18].

Mixtures of surfactants, polymers, and alkalis, such as ASP, can be used for the same purposes. Microbial EOR involves injecting microorganisms into a reservoir that grows rapidly under specific environmental conditions, developing variant metabolites that can mobilize oil[19]. These microorganisms can influence the chemical and physical properties of a reservoir, and their growth depends on several factors, including porosity, permeability, and reservoir conditions[20]. Microbial EOR uses biomass or biopolymers to selectively plug high-permeability zones or reduce the IFT using solvents or biosurfactants[19]. In contrast to Chemical EOR, Microbial EOR is more cost-effective, independent of oil prices, and environmentally friendly[21]. Gas EOR techniques employ the injection of various gases primarily to maintain reservoir pressure and enhance oil mobility; these gases can include N_2, CO_2, hydrocarbons (e.g., methane or ethane), and gas mixtures such as N_2/CO_2, depending on the nature of the reservoir. However, CO_2 is the most commonly used gas. When injected in its supercritical state, it dissolves in the oil phase and mobilizes oil towards the production well[22]. In particular, even if CO_2 were injected in the gaseous phase, it would be in its supercritical state due to the low critical properties of CO_2,, with critical pressure $P_c = 1069.51$ psi and critical temperature $T_c = 30.97$°C. These values are, in general, lower than reservoir conditions[23]. The gas injected into a reservoir undergoes either First Contact Miscibility (FCM) or Multiple Contact Miscibility (MCM)[24,25]. The FCM indicates that the injected fluid is instantly mixed with oil in all proportions upon first contact and is affected by the reservoir pressure and temperature. In contrast, in MCM, the fluid is injected to undergo multiple contacts with the oil, gradually reducing the IFT until they are mixed[26]. In particular, CO_2 injected into the oil with multiple contacts until it forms an oil bank is considered an MCM process; that is, when a mixture of both fluids is formed[25].

The exact definition of the MMP varies across the literature. However, MMP can be defined as the pressure value at 1.2 PV of injected gas or when the RF reaches 90%[27]. Similarly, the MMP is the minimum pressure required to achieve miscibility between oil and gas and is influenced by the surrounding conditions through dynamic interactions[28,29]. Reaching the MMP is crucial for establishing miscible CO_2 flooding and achieving the highest possible oil recovery[29]. The MMP is influenced by simultaneous vaporization and condensation, with oil swelling reaching up to 60%, thereby increasing the OOIP saturation depending on pressure, temperature, oil composition, and CO_2 mole fraction. The IFT and oil viscosity factors are also reduced, which facilitates oil flow[30]. However, miscible flooding cannot always be obtained, particularly in reservoirs with high temperatures where higher injection pressures exceed the formation fracture pressure[31]. Several approaches for measuring the MMP value have been proposed. The slim tube test (STT) is one of the most accurate and reliable methods in the industry[29].

A schematic of the STT test setup is shown in Figure 1. The setup comprises a coiled slim tube made of stainless steel that is internally packed with different materials, such as glass beads or silica sands, along with different mesh numbers, a positive displacement pump, a burette to collect the oil outflow, a back-pressure regulator, a syringe pump, and a gas chromatographer to measure the gas outflow composition and a gas flow meter[29,32]. Previous studies have suggested that tubes with smaller diameters are preferable because larger diameters may cause undesired influences on established miscible flooding[33]. An innovative protocol has been proposed[34] to accurately determine the MMP by chromatographic separation of the produced gas. The study suggests that the composition of effluent gas, specifically the C_1/C_3 ratio, can be tracked. This ratio indicates the presence of a methane bank during immiscible injection and its eventual disappearance. The experimental runs were reduced to approximately four times, and during each run, gas samples were collected and analyzed to obtain the C_1/C_3 ratio, which was then recorded at different pressure levels. A plot of C_1/C_3 vs. the injected Pore Volume was analyzed, and the methane area was calculated, with the process repeated several times until the area converged to zero as the MMP approached. However, this method incurs additional costs due to effluent gas analysis required to obtain the C_1/C_3 ratio. Other authors[35] have investigated the effect of the injection rate. In general, as the injection rate increased, the MMP value increased. However, their findings showed that the MMP decreased as the injection rate increased. Increasing tube length, on the other hand, decreases MMP.

Alternatively, the VIT technique can be used to determine MMP[37]. This technique is based on the idea that, when the miscibility point is reached, whether through FCM or MCM, the IFT value drops to zero; therefore, the pressure point can be considered as the MMP[38]. The initial setup of the VIT technique included a high-pressure high-temperature (HPHT) cell, pressure pumps, an oven, a back-pressure regulator, and a camera system to capture the drop profile using ADSA software, as shown in Figure 2. He used rainbow stock-tank oil (STO), Gilwood STO, propane, and ethane as solvents. In addition, to determine the effectiveness and accuracy of the VIT method, several STT experiments across four case studies were conducted (each solvent was used twice with each oil sample). The findings indicated that VIT is a viable and efficient technique that provides a rapid and reliable estimate of MMP. For instance, STT reported MMP values of 1044.27–1073.28 psi, whereas VIT

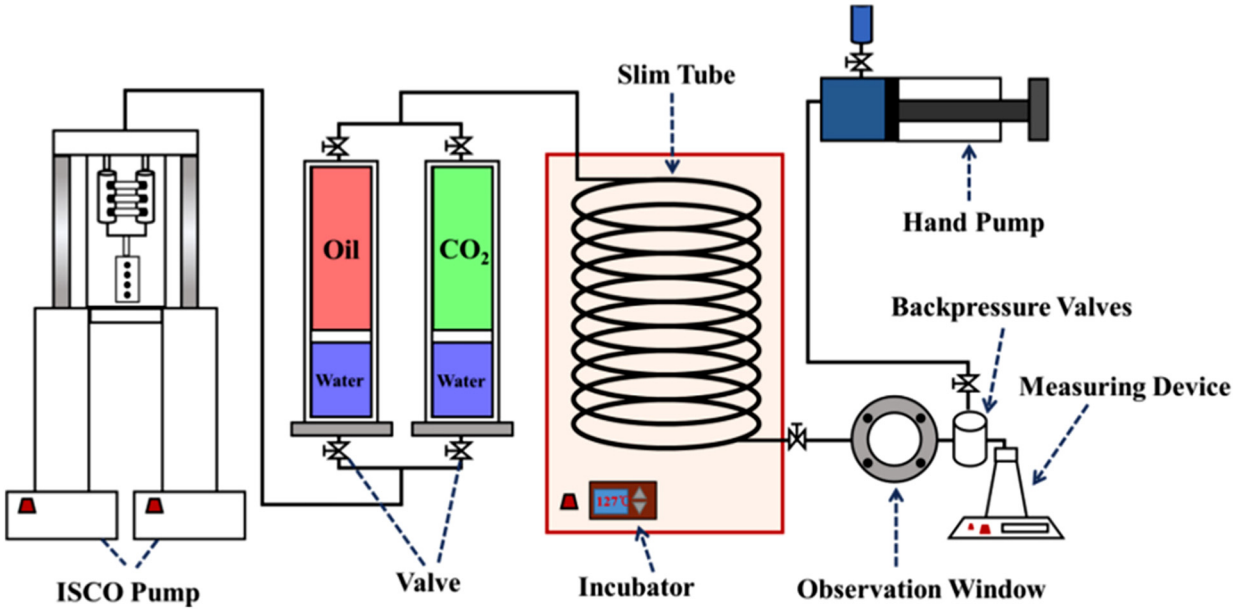

Figure 1. Schematic of the STT test setup. Adapted from Almobarak[36]

yielded 1092.134 psi when Gliwood STO was tested with ethane gas as a solvent, thereby demonstrating the accuracy and agreement between the two techniques. However, with Rainbow STO and ethane as the solvent, VIT yielded a MMP of 2646.94 psi, whereas using STT yielded 1624.423 psi. The considerable difference in values can be attributed to the asphaltene onset at the crude oil–gas-oil interface, which slows the drop in the IFT and disrupts the linear trend. In a subsequent study, the effect of different gas compositions on the MMP using the VIT technique was investigated[38]. The study considered Terra Nove live oil with 3 different gases at a reservoir temperature of 96°C. In addition, Different MMP measurements, such as VIT and STT, were compared[39]. The study used CO_2 (99.9% pure) as the injection fluid (solvent phase) and crude oil with an API of 41.38 from the Air Benakat Formation. The study revealed that the MMP values estimated by VIT and STT differ slightly at high temperatures and are considered negligible for EOR purposes. In contrast, at low temperatures, discrepancies were present between the MMP values of STT and VIT.

Moreover, the Rising Bubble Apparatus (RBA) can be utilized to measure the MMP using a see-through glass tube. The experimental setup of the RBA mainly comprises a visible glass tube, high-pressure, and high-temperature cell, which includes a glass tube, a needle to inject gas bubbles, and a camera to capture the bubble's behavior as it rises through oil, pumps, and fluid cylinders[29,40]. In this method, a gas drop is introduced into the oil medium, and the drop travels from the bottom to the top of the vessel under gravity and density differences, and the dynamic

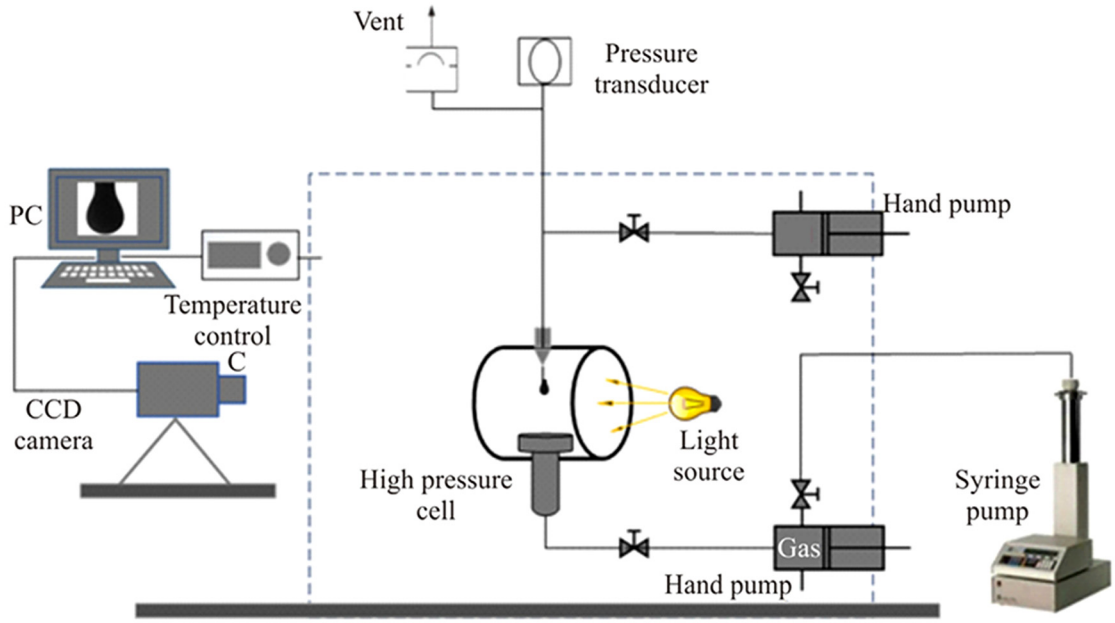

Figure 2. VIT experimental setup used to measure IFT values at high temperatures and pressures. Adapted from Almobarak et al[31]

Table 1. *Past studies on reduction of MMP using different additives and different methods to evaluate MMP*

Author	Oil Properties	Temperature	Additives	MMP Measuring Method	Key Outcomes
Yang et al. (2019) [43]	Asphaltene 1.76%, resins 16.87%, aromatics 27.86%, saturates 53.48%	343.15 K	Individual and combination of alcohols (1-butanol, 1-pentanol, 1-hexanol)	VIT	Solubility of CO_2 increased by 20.7%, MMP reduced by 9.21%
Liu et al. (2019) [44]	Density 0.85 g/cm^3, viscosity 9.8 mPa•s	343.15 K	Petroleum ether	VIT	MMP reduced by 16%
Zhang et al. (2020) [45]	Density 0.87 g/cm^3, viscosity 23.7 mPa•s	333.15 K	CO_2 soluble surfactants and ethanol	VIT	MMP was reduced by 26.79-34.52%
Zhao et al. (2021) [46]	Viscosity 1.88 mPa•s Density of C_{7+} is 0.8971 g/cm^3	381.65 K	Citric acid isobutyl ester, citric acid isopentyl ester (Oil soluble)	STT (packing material: quartz sand)	MMP reduction by 15.96-16.84%

profile of the drop as it moves upward is captured. The IFT was determined based on the shape of the drop and the way it travels.

The MMP depends on several factors, including reservoir conditions, crude oil composition, and injection gas composition. For instance, the reservoir temperature increases the MMP value because CO_2 solubility in oil decreases with temperature. Oil and gas compositions are also crucial because lighter oil components (C_1-C_6) can be dissolved by CO_2 at a lower pressure than heavier components. In contrast, injected gas compositions or mixtures affect substantially [28,31,41,42]. Previous studies have explored the effects of different additives on MMP reduction. Other studies have reported a considerable reduction in MMP, whereas other chemicals were ineffective to a high degree.

The relationship between the MMP and oil recovery factor can be linked back to Eq. 1. The overall sweep efficiency incorporates both microscopic and macroscopic sweep efficiencies. To increase the microscopic sweep efficiency, the IFT between phases must be reduced. As explained earlier, under miscible conditions, IFT is typically approximately 0. Hence, by realizing miscibility and reducing the IFT, the microscopic sweep efficiency is improved, thereby increasing the overall sweep efficiency.

This study investigated the effect of chemically assisted CO_2 flooding on MMP reduction using specific types of chemicals, including ionic liquids or surfactants. The VIT technique is used to measure the IFT values, allowing estimation of the MMP value. Understanding MMP behavior and its response to different chemicals is crucial to increase flooding efficiency and achieve a miscible state in challenging environments, such as in shallow or high-temperature reservoirs, and to promote injection economics by reducing costs when high pressure is needed to achieve MMP. Previous attempts to reduce the MMP are listed in Table 1.

2. METHODOLOGY

2.1. Materials . The crude oil sample used was Uthmania Crude Oil from Ghawar Field in Eastern Saudi Arabia, available at the Center of Integrated Petroleum Research (CIPR). The specific oil properties at 25°C are listed in Table 2. Pure toluene was used to remove potential contamination. CO_2 with a purity of >99% was used. Ionic Liquid 360 (IL360) Ionic Liquid 690 (IL690) were used as chemical additives to evaluate their impact on MMP. SARA Analysis was performed using thin-layer chromatography (TLC) and Flame Ionization Detection (FID) in three steps. First, 1 µL of oil was diluted in dichloromethane, and 3-step elution was performed using TLC. Then, the detection of distinct groups within the rod was performed using FID as per standard IP 469.

2.2. Apparatus.

2.2.1. IFT setup. A drop shape analyzer (model: DSA100HP690) was used to measure IFT at high pressures and temperatures. This system can be used to determine the interfacial tension between CO_2 and oil, using a pendant drop. The setup comprises a CO_2 cylinder, an ISCO syringe pump (Teledyne ISCO 260D with a precision of 0.5%), a high-pressure cell, a digital camera to capture the drop shape, a manual positive-displacement pump, heater elements, and a data-controlling unit, as shown in Figure 3. CO_2 was introduced into the pressure chamber using a syringe pump at a specific pressure. The high-pressure vessel comprised one or two glass windows that allow light to pass through, a 0.857-mm radius needle installed on the ceiling, and 3- outlet ports. The chamber was covered with a heating jacket to ensure improved insulation. A high-resolution camera (1920x1200 pixels) was installed to capture the drop shape images. The camera can be controlled using the zoom,

Table 2. *Uthmania oil properties*

Density (g/cc)	0.8724
Viscosity (cP)	15.1
°API	28.75
SARA	Saturates: 36.2 Aromatics: 50.0 Resins: 11.0 Asphaltenes: 2.80

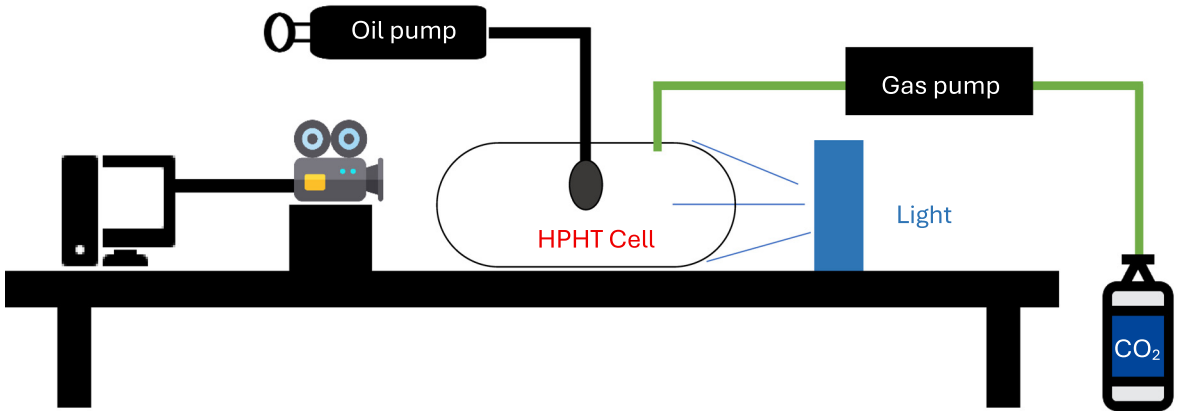

Figure 3. Schematic of IFT equipment

focus, and view angle. The obtained data were analyzed using advanced image software analysis. An electrical heating unit was also installed in the drop-shaped analyzer, with the temperature controlled by a digital controller. The pressure was controlled by pumps, and the gauge displayed the cell pressure value.

2.2.2. Density device. The equipment to measure density included a controller, a cylinder in which oil was poured and pressurized, and a manual pump to pressurize the oil specimen. As density is a significant factor in this study, an Anton Parr 4500M density meter was used. This density meter has high accuracy, ensuring high precision (density measurements reported to five decimal places). In addition, the density device is connected to a heating system that allows adjustment of the desired temperature. The manual pump was controlled by a manual rod connected to a cylinder containing the oil sample, and a pressure reading appeared on the controller. The density meter has a built-in mechanism that corrects the density measurements based on the viscosity of the fluid, calibration data, and typical fluid behavior.

2.3. Procedures.

2.3.1. Density measurements. First, the entire density setup was thoroughly cleaned. First, the cylinder was opened, the cap was removed, and the cylinder was cleaned with DI water. Subsequently, the entire setup, including the specimen (cylinder) and the density tool, was flooded with toluene to ensure that oil traces and impurities were completely cleaned and removed. Then, nitrogen flooding was performed throughout all parts to remove any residual toluene, and the setup was fully dried once the density reading was that of air. After cleaning the setup, oil was transferred to the specimen, and the temperature was adjusted to 80°C. The oil sample was maintained for a certain time until it reached and stabilized at a specified temperature. Then, the pressure was increased in 200-psi increments from 200 psi to 3000 psi.

2.3.2. IFT measurements. Before conducting any tests, the high-pressure, high-temperature cell was cleaned with toluene to remove any remaining traces of oil. Similarly, the specimen containing the liquid sample was treated with acetone and toluene to remove traces of the oil sample and any other impurities. Typically, the manual oil pump is treated by injecting and draining toluene more than 15 times until the drained toluene is completely transparent and clear, without any dust or residue. The cells were then flooded with nitrogen for complete drying. Pressure was applied from a CO_2 tank, and the temperature was set by the heating jacket and left for several hours to stabilize and ensure that all traces of liquids and impurities were vaporized. Subsequently, the system was isolated and the system was inspected for leaks and loose fittings. Finally, the system was vacuumed. The cell was filled with CO_2 to conduct the experiments. CO_2 was injected into the chamber, and the pressure was maintained at the desired value. Once completed, an oil drop was formed by manually injecting oil from an oil specimen through the needle connected to the ceiling of the cell. The drop should be stable for some time, and the software should directly calculate the IFT value. ADSA was used to calculate IFT measurements.

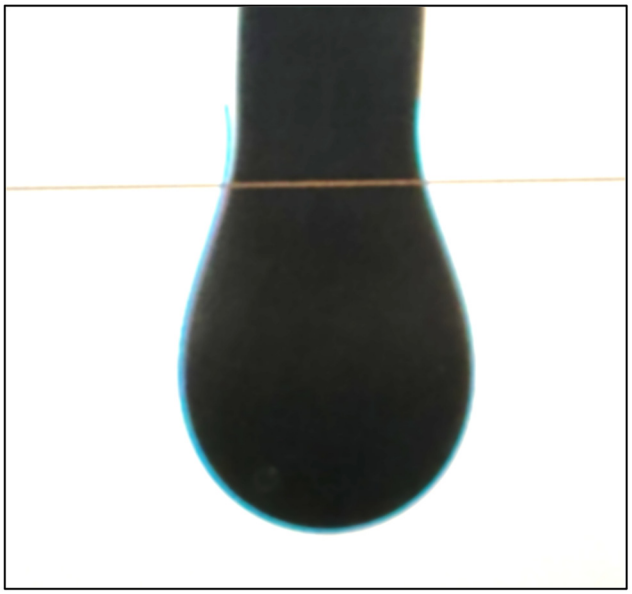

Figure 4. Drop Shape during IFT test. The blue curve must match the pendant drop so that ADSA calculates IFT

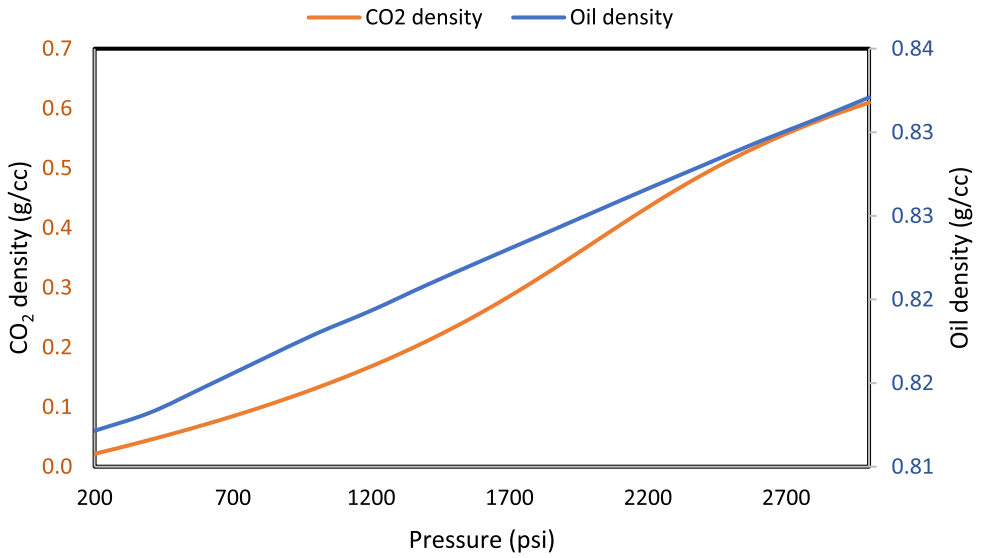

Figure 5. Oil and CO_2 densities as function of pressure

This technique is considered accurate and reliable for evaluating the drop shape over a wide range of pressures and temperatures. ADSA depends on the numerical matching of the drop-shaped geometry with the Laplace equation (Eq. 2):

$$\Delta p = \sigma \left(\frac{1}{R_1} + \frac{1}{R_2} \right) \tag{2}$$

where Δp is the pressure difference between two phases, σ is IFT (mN/m), and R_1 and R_2 are the principal radii of curvature. Figure 4 illustrates an oil pendant drop during the real test; it can be observed that the blue curve that is generated by the software matches the drop curvature. Also, the orange or red line shown in the middle is the tip of the needle. As stated before, the VIT technique was used to calculate the MMP between oil-CO_2 phases because it provides accurate results within a shorter time than slim-tube experiments. The IFT values were extrapolated to zero to obtain MMP. The evaluated range was from 200 psi to 3000 psi at 80°C. No repeated measurements were performed; therefore, standard deviation and uncertainty could not be quantified.

3. RESULTS AND DISCUSSION

3.1. Density Measurements. The obtained density values are listed in Table 3. Figure 5 presents the variation in oil and CO_2 with pressure at 80°C. Oil density increases with pressure because less volume is occupied by the same amount of oil in the testing vessel, following the typical trend and fluid behavior. The CO_2 densities were obtained from the NIST WebBook. The data provided were highly accurate and reliable, as they have been used in several studies. Similarly, the gas density increased

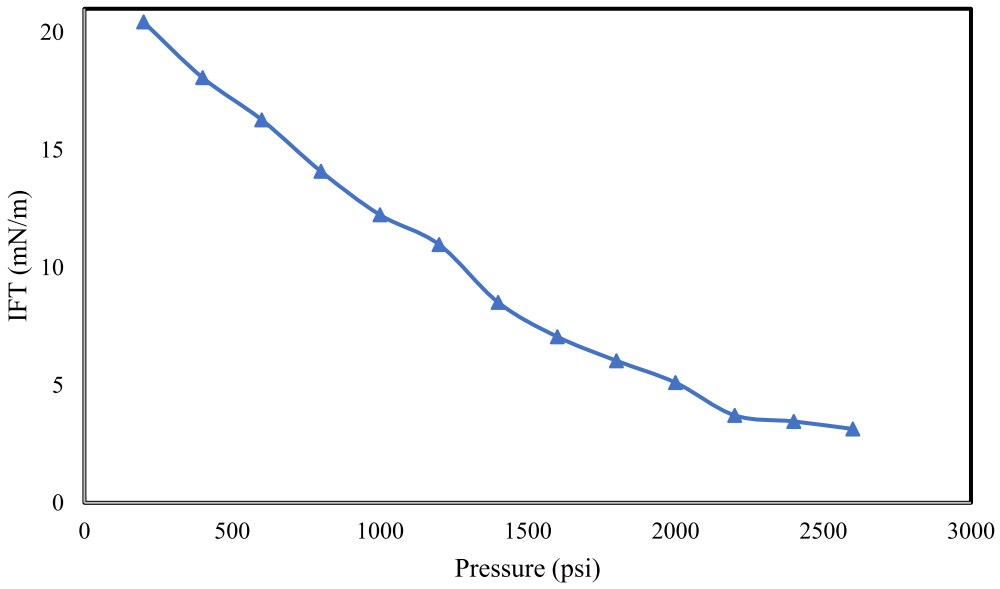

Figure 6. IFT values between phases of pure oil and CO_2 at 80°C

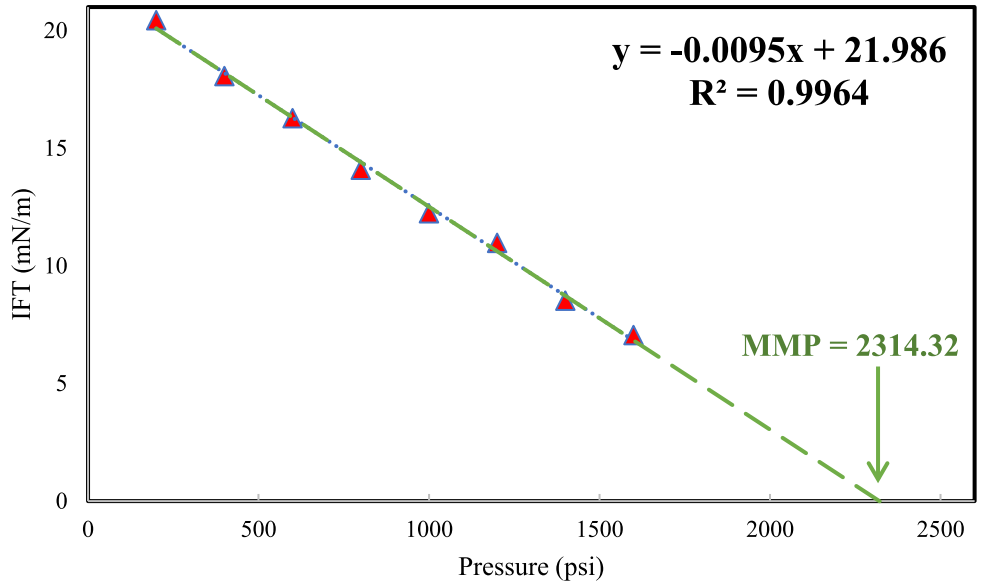

Figure 7. MMP for base case at 80°C

with increasing pressure, while the temperature remained constant. For comparison, Figure 5 shows both densities of gas and oil with increasing pressure at a constant temperature of 80 °C.

3.2. IFT and MMP Determination. IFT tests were performed using DSA100 manufactured by Kruss in Germany. To determine the effectiveness of all chemicals, the first measurements focused on obtaining a baseline: pure oil and pure CO_2. The IFT values are shown in Figure 6. As pressure increases, the IFT decreases because higher pressure enhances CO_2 solubility in the oil phase through continuous mass transfer between the phases[47]. Maintaining the drop on the needle at high pressures (2000 psi and above) is challenging because CO_2 counteracts the oil drop and attempts to expand even inside the needle. The IFT values decreased with increasing pressure and eventually approached a plateau. This decreasing trend is consistent with the literature[47].

From the IFT value plot for the baseline, the MMP was estimated by extrapolating the trendline through the decreasing IFT values, with the abscissa corresponding to the MMP. However, determining the last point until IFT stabilization occurs must be systematic. Therefore, the Least Correlation Coefficient (LCC) R^2, i.e., the correlation coefficient, was used in this study to determine the best-fitting trendline and the MMP, as reported in the literature[48]. The VIT method assumes that at miscibility, the IFT must be approximately zero, and consequently, the trendline must be extended to zero[37]. The best *LCC* was 0.9964, yielding an **MMP** of **2314.32** psi, as shown in Figure 7. In general, at this temperature, various chemicals and solvents fail to reduce the MMP owing to the extreme conditions of the experiments.

Similarly, IFT measurements were performed for the first additive, IL360, with a concentration of 0.02%. The results are shown in Figure 8. The initial IFT at 200 psi was 15.38 mN/m, approximately 24.76% lower than the baseline value at the same pressure,

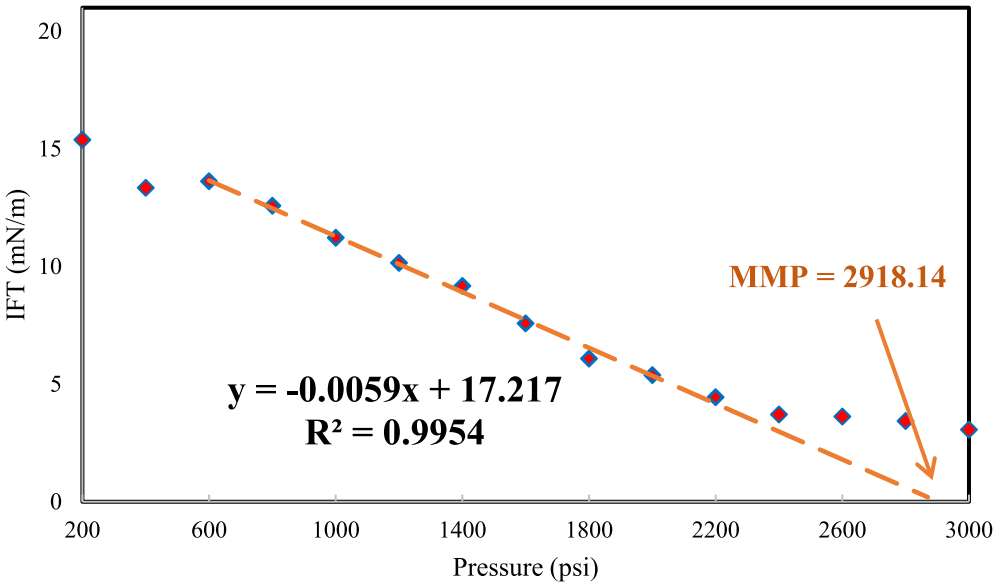

Figure 8. IFT values for IL360 with 0.02% concentration at 80°C

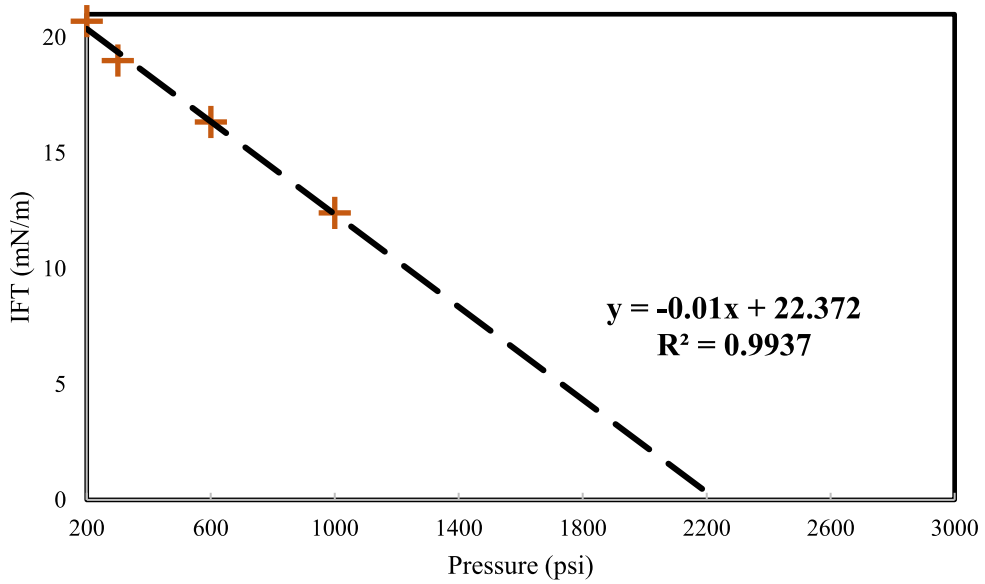

Figure 9. IFT measurements determined for second additive IL690 at 80°C

indicating a positive sign. However, as the measurements progressed, the IFT values increased with a positive gradient and then decreased with a lower slope from 200 to 400 psi. The initially obtained trend can be attributed to the positive effect of the additive when first introduced to the system, thereby showing a drop in IFT values. However, the IFT increased again owing to the IL360 degradation at the high temperature. Therefore, IL360 is considered unsuitable candidate to operate at a temperature of 80 °C.

Subsequently, a second chemical additive (IL690) was tested. The chemical solution was prepared at the same concentration as that used for the first additive (IL360) (0.02 %). The entire setup was treated and cleaned, including the flowing tubing, HPHT cell, pump, and all valves with water and toluene, and flushed with CO_2. The results for IL690 are shown in Figure 9. Note that the IFT and baseline values, when examined closely, are almost the same. Once extrapolated, the resulting MMP was 2237.2 psi, which was 3.33% lower than the baseline. The reduction is minimal compared to the previously reported values[43–46], within 20–50% reduction considered effective. However, unlike the first additive, it exhibited a trend similar to that of the baseline, thereby resembling its reproducibility. A comparison of the measured IFT for the baseline and the chemically assisted cases is shown in Figure 10. Notably, relative difference for IL360 was initially positive (reduction); however, then the trend reversed to negative as higher IFT values were obtained. For IL690, the initial values were closer to or slightly above the baseline, and the gradient was steeper for the extrapolated line, indicating a reduction of 3.33%.

3.3. MMP Correlations. As discussed in the previous sections, the MMP is affected by multiple factors, including oil and injected gas compositions, and reservoir temperature[49]. In addition, the applicability of these correlations depends on the range specified by the developers. Hence, several correlations in

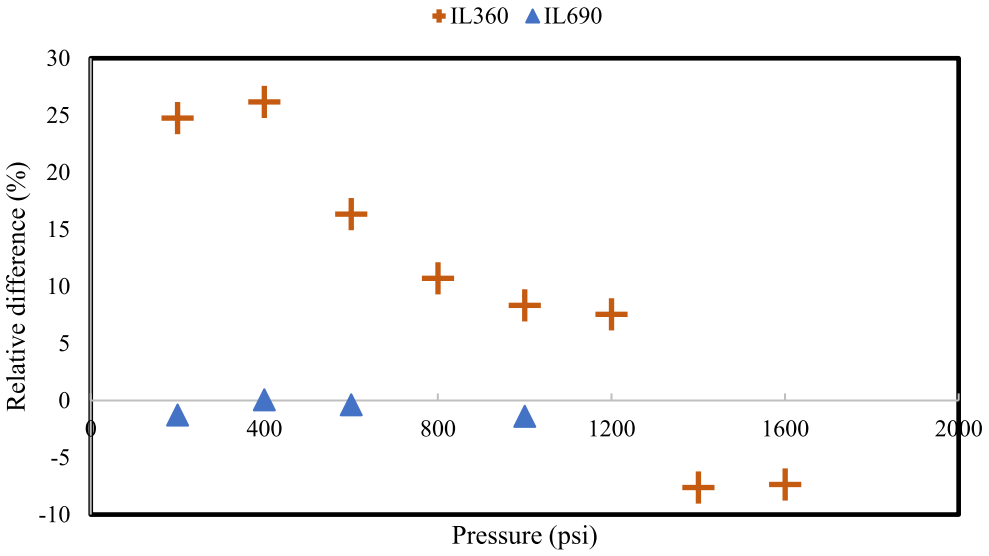

Figure 10. Comparison of relative difference between IFT for base case and chemical assisted cases

Table 3. *Oil density measurements at 80°C*

Pressure (psi)	Density (g/cc)
200	0.81215
400	0.81323
600	0.81479
800	0.81638
1000	0.81795
1200	0.81934
1400	0.82086
1600	0.82232
1800	0.82375
2000	0.82519
2200	0.82663
2400	0.82803
2600	0.82943
2800	0.83073
3000	0.83209

the literature that consider multiple factors to obtain an accurate and valid estimate of the MMP, such as MW_{5+}, MW_{7+}, and X_{vol}/X_{int} [50,51]. Among them, two widely applied correlations [52,53] for estimating MMP in pure CO_2-oil systems were benchmarked against experimental tests, as in previous studies [54]. The Yellig–Metcalfe [52] correlation was originally developed based on various oil compositions and temperatures, although no composition terms appeared in their correlation. The oils consisted of a light fraction mainly composed of C_1, an intermediate fraction comprising hydrocarbons with molecular weights of C_2-C_6, and a heavy fraction comprising C_{7+} [52]. In a later study [53], the Yellig and Metcalfe method was implemented for CO_2-oil systems by varying oil samples and gas-oil ratios at three temperatures: 32, 41, and 49°C**.** Further correlations to estimate the MMP while accounting for the effects of MW_{5+}, MW_{7+}, and X_{vol}/X_{int} have been reported [55,56]. Note that the molecular weight of C5+ and C7+ must be considered because oil composition significantly affect the MMP value, especially when the test is performed above 48.9°C [54,57]. For instance, the mole fraction of volatile components increases MMP. In contrast, the mole fraction of the intermediate components decreased the MMP. A summary of the results from previous studies is presented in Table 4. Molecular weights are required to apply all of the correlations mentioned. Therefore, the correlation proposed by Holtz *et al.* [58] for calculating MW_{C5+} is presented in Eq. 3 based on API degrees. Furthermore, ratio of X_{vol}/X_{int} was calculated as suggested by Alston *et al.* [59], as shown in Eq. 4.

$$MW_{C_{5+}} = \left(\frac{7864.9}{^{\circ}API}^{0.9628}\right) \tag{3}$$

$$\frac{X_{vol}}{X_{int}} = \frac{120}{^{\circ}API} \tag{4}$$

Once all required parameters are calculated, the MMP is estimated using the empirical correlations listed in Table 4. The results are summarized in Table 5 along with a comparison shown in Figure 11. The observed differences in these correlations range from 10 to 30%. Yellig & Metcalfe method provided the most accurate correlation for the baseline, with a difference of 2.91%. Following this, Li et al [55] model provided a difference of 10.29%, followed by Orr & Jensen [53] with 15.65%, and Emera & Sarma, [56] with 29.25 %. Li *et al.* reported a larger percentage difference compared to Yellig & Metcalfe, even after accounting for oil composition. This result can be attributed to how X_{vol}/X_{int} was calculated or to the correlation used to estimate MW_{C5+}. Typically, an error of 1–5% is acceptable, depending on the desired accuracy or threshold specified by the study. The applicability of each correlation depends on the context and the available parameters. For example, several correlations require a specific solution–gas ratio. These correlations were excluded from this study because the oil samples used are dead oils.

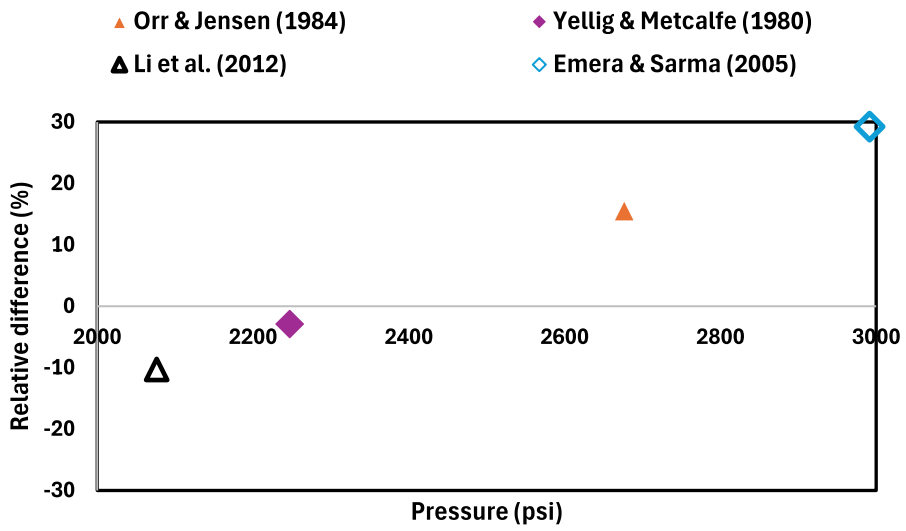

Figure 11. Empirical correlations to estimate MMP suggested by different scholars

Table 4. *Experimental conditions*

No.	Author(s)	Correlation	Parameters
1	Yellig and Metcalfe (1980) [52]	$MMP = 1883.717 + 2.2518T + 0.018T^2 - \frac{103949.93}{T}$	T (°F)
2	Orr & Jensen (1984) [53]	$MMP = 0.101386e^{\left(10.91 \frac{2015}{255.372+0.5556(1.8T+32)}\right)}$	T (°F)
3	Li *et al.* (2012) [55]	$MMP = 7.30991 \times 10^{-5} (\ln[1.8T]^{5.33647} (\ln MW_{C_{5+}}^{2.08836}) (1 + X_{vol}/X_{int})^{0.201658}$	T (°C), X_{vol}, X_{int}, MW_{C5+}
4	Emera & Sarma (2005) [56]	$MMP = 7.43497 \times 10^{-5} (1.8T + 32)^{1.1669} (MW_{C_{5+}})^{1.201}$	T (°C), MWC_{5+}

Table 5. *MMP value determined based on correlations*

Correlation	MMP (psi)
Yellig & Metcalfe (1980) [52]	2246.98
Orr & Jensen (1984) [53]	2676.45
Li *et al.* (2012) [55]	2076.28
Emera & Sarma (2005) [56]	2991.35

4. CONCLUSIONS

This study focused on improving CO2-flooding by adding chemical additives (ionic liquids, IL) to lower the MMP. Based on the experimental and/or analytical results, the following key conclusions can be drawn:

- Two chemical additives were tested to investigate their impact on the MMP. The VIT technique was applied to evaluate MMP based on the assumption that miscibility is achieved when the IFT approaches zero.
- The results suggest that the first additive (IL360) was only partially effective at the beginning of the experiment. Subsequently, because of the high temperature, the surfactant failed to maintain a low IFT trend, although the first two points were approximately 25% lower than those of the reference or base case.
- However, the impact of the second additive was minimal and yielded almost the same IFT values as those of the base case, with minor differences. When extrapolated, the recorded abscissa was 3.33% lower than the MMP for the base case, which is considered a small reduction.
- To compare the MMP from different correlations, they were benchmarked against the experimental values determined for the base case. There are various correlations to estimate the MMP with many parameters that are involved in each correlation because the MMP depends on multiple factors, as discussed in earlier sections.
- Four different empirical correlations were evaluated in this study. The minimum relative difference obtained by the aforementioned correlations was 2.91% from the reference case using the Yellig & Metcalfe correlation.
- This study contributes to oil production enhancement techniques where gowing energy demand can be fulfilled. Further investigation might consider screening more ionic liquids based on operational temperature whilst taking cost into account, and the effect of combinations of different ionic liquids may be explored.

AFFILIATIONS AND AUTHOR DETAILS

Undergraduate Author

Abdullah Almahasnah – *Department of Petroleum Engineering, King Fahd University of Petroleum & Minerals, Dhahran 31261, Saudi Arabia*; 0009-0001-6339-7362
Email: mahasnah@stanford.edu

Corresponding Author

Arshad Raza – *Research Mentor, Assistant Professor, Department of Petroleum Engineering, King Fahd University of Petroleum & Minerals, Dhahran 31261, Saudi Arabia*; 0000-0001-7706-1002
Email: arshad.raza@kfupm.edu.sa

ACKNOWLEDGEMENTS

The authors would like to acknowledge the support provided by the Department of Petroleum Engineering and the Center for Integrative Petroleum Research (CIPR) at King Fahd University of Petroleum and Minerals (KFUPM). The authors also extend their appreciation to Dr. Muhammad Shahzad, Eng. Ahmad Mahboob, and Eng. Mobeen Murtaza for their continuous guidance and assistance in this project.

REFERENCES

(1) World. World Energy Outlook 2023 – Analysis - IEA. *IEA* https://www.iea.org/reports/world-energy-outlook-2023 (2023).

(2) Zhang, J. Energy access challenge and the role of fossil fuels in meeting electricity demand: Promoting renewable energy capacity for sustainable development. *Geosci. Front.* **15**, 101873 (2024).

(3) Bagherian, M. A. & Mehranzamir, K. A comprehensive review on renewable energy integration for combined heat and power production. *Energy Convers. Manag.* **224**, 113454 (2020).

(4) Olabi, A. & Abdelkareem, M. A. Renewable energy and climate change. *Renew. Sustain. Energy Rev.* **158**, 112111 (2022).

(5) Mohammadi, M. H., Kulakhmetovna, Y. A. & Joia, R. An overview of oil recovery techniques: From primary to enhanced oil recovery methods. *J. Res. Appl. Sci. Biotechnol.* **3**, 291–301 (2024).

(6) Muggeridge, A. *et al.* Recovery rates, enhanced oil recovery and technological limits. *Philos. Trans. R. Soc. Math. Phys. Eng. Sci.* **372**, 20120320 (2013).

(7) Nwidee, L. N., Theophilus, S., Barifcani, A., Sarmadivaleh, M. & Iglauer, S. EOR Processes, Opportunities and Technological Advancements. in *InTech eBooks* (2016). doi:10.5772/64828.

(8) Antolinez, J. D., Miri, R. & Nouri, A. In situ Combustion: A Comprehensive review of the current state of knowledge. *Energies* **16**, 6306 (2023).

(9) Mokheimer, E. M. A. *et al.* A Comprehensive Review of Thermal Enhanced Oil Recovery: Techniques Evaluation. *J. Energy Resour. Technol.* **141**, (2018).

(10) Alvarado, V. & Manrique, E. Enhanced Oil Recovery: An update review. *Energies* **3**, 1529–1575 (2010).

(11) Santos, R. G., Loh, W., Bannwart, A. C. & Trevisan, O. V. An overview of heavy oil properties and its recovery and transportation methods. *Braz. J. Chem. Eng.* **31**, 571–590 (2014).

(12) Pothula, G. K., Vij, R. K. & Bera, A. An overview of chemical enhanced oil recovery and its status in India. *Pet. Sci.* **20**, 2305–2323 (2023).

(13) Yousefvand, H. & Jafari, A. Enhanced Oil Recovery Using Polymer/nanosilica. *Procedia Mater. Sci.* **11**, 565–570 (2015).

(14) Abidin, A., Puspasari, T. & Nugroho, W. Polymers for enhanced oil recovery technology. *Procedia Chem.* **4**, 11–16 (2012).

(15) Bashir, A., Haddad, A. S. & Rafati, R. A review of fluid displacement mechanisms in surfactant-based chemical enhanced oil recovery processes: Analyses of key influencing factors. *Pet. Sci.* **19**, 1211–1235 (2021).

(16) Aisha, N. *et al.* Wetting the Surface: A Deep Dive into Chemistry and Applications of Surfactants. *Clean. Chem. Eng.* **100197**, (2025).

(17) Mandal, A. Chemical flood enhanced oil recovery: a review. *Int. J. Oil Gas Coal Technol.* **9**, 241 (2015).

(18) Mayer, E., Berg, R., Carmichael, J. & Weinbrandt, R. Alkaline injection for enhanced oil recovery - a status report. *J. Pet. Technol.* **35**, 209–221 (1983).

(19) Sharma, N., Lavania, M., Singh, N. & Lal, B. Microbial Enhanced oil Recovery: an overview and case studies. in *IntechOpen eBooks* (2022). doi:10.5772/intechopen.106641.

(20) Yernazarova, A. *et al.* Exploring the use of microbial enhanced oil recovery in Kazakhstan: a review. *Front. Microbiol.* **15**, (2024).

(21) Niu, J., Liu, Q., Lv, J. & Peng, B. Review on microbial enhanced oil recovery: Mechanisms, modeling and field trials. *J. Pet. Sci. Eng.* **192**, 107350 (2020).

(22) Ozowe, N. W., Daramola, N. G. O. & Ekemezie, N. I. O. Innovative approaches in enhanced oil recovery: A focus on gas injection synergies with other EOR methods. *Magna Sci. Adv. Res. Rev.* **11**, 311–324 (2024).

(23) Wise, M. & Chapoy, A. Carbon dioxide solubility in Triethylene Glycol and aqueous solutions. Fluid Phase Equilibria,419,39–49. (2016) doi:10.1016/j.fluid.2016.03.007.

(24) Luo, E., Fan, Z., Hu, Y., Zhao, L. & Wang, J. An evaluation on mechanisms of miscibility development in acid gas injection for volatile oil reservoirs. *Oil Gas Sci. Technol. – Rev. D'IFP Energ. Nouv.* **74**, 59 (2019).

(25) Feng, H. *et al.* Assessment of miscibility effect for CO 2 flooding EOR in a low permeability reservoir. *J. Pet. Sci. Eng.* **145**, 328–335 (2016).

(26) Kumar, N., Sampaio, M. A., Ojha, K., Hoteit, H. & Mandal, A. Fundamental aspects, mechanisms and emerging possibilities of CO2 miscible flooding in enhanced oil recovery: A review. *Fuel* **330**, 125633 (2022).

(27) Jacobson, H. Acid gases and their contribution to miscibility. *J. Can. Pet. Technol.* **11**, (1972).

(28) Song, G., Meng, Y., Zhang, C., Zhao, Z. & Yang, Q. Comprehensive Review of the Determination and Reduction of the Minimum Miscibility Pressure during CO2 Flooding. *ACS Omega* **9**, 14747–14765 (2024).

(29) Chen, Z., Chen, J. & Zhang, X. A comprehensive review of minimum miscibility pressure determination and reduction strategies between CO2 and crude oil in CCUS processes. *Fuel* **384**, 134053 (2024).

(30) Zhang, N., Yin, M., Wei, M. & Bai, B. Identification of CO2 sequestration opportunities: CO2 miscible flooding guidelines. *Fuel* **241**, 459–467 (2018).

(31) Almobarak, M. *et al.* A review of chemical-assisted minimum miscibility pressure reduction in CO2 injection for enhanced oil recovery. *Petroleum* **7**, 245–253 (2021).

(32) Zhang, K. & Gu, Y. Two different technical criteria for determining the minimum miscibility pressures (MMPs) from the slim-tube and coreflood tests. *Fuel* **161**, 146–156 (2015).

(33) Holm, L. W. & Josendal, V. A. Effect of oil composition on Miscible-Type displacement by carbon dioxide. *Soc. Pet. Eng. J.* **22**, 87–98 (1982).

(34) Mogensen, K. A novel protocol for estimation of minimum miscibility pressure from slimtube experiments. *J. Pet. Sci. Eng.* **146**, 545–551 (2016).

(35) Ahmad, W., Vakili-Nezhaad, G., Al-Bemani, A. S. & Al-Wahaibi, Y. Uniqueness, repeatability analysis and comparative evaluation of experimentally determined MMPs. *J. Pet. Sci. Eng.* **147**, 218–227 (2016).

(36) Almobarak, M. *et al.* Chemical-assisted MMP reduction on methane-oil systems: Implications for natural gas injection to enhanced oil recovery. *Petroleum* **10**, 101–108 (2024).

(37) Rao, D. N. A new technique of vanishing interfacial tension for miscibility determination. *Fluid Phase Equilibria* **139**, 311–324 (1997).

(38) Rao, D. N. & Lee, J. Application of the new vanishing interfacial tension technique to evaluate miscibility conditions for the Terra Nova Offshore Project. *J. Pet. Sci. Eng.* **35**, 247–262 (2002).

(39) Abdurrahman, M. *et al.* Minimum CO_2 Miscibility Pressure Evaluation using Interfacial Tension (IFT) and Slim-tube Hybrid Tests. *ACS Omega* **8**, 8703–8711 (2023).

(40) Zhang, K. & Gu, Y. New qualitative and quantitative technical criteria for determining the minimum miscibility pressures (MMPs) with the rising-bubble apparatus (RBA. *Fuel* **175**, 172–181 (2016).

(41) Choubineh, A., Helalizadeh, A. & Wood, D. A. The impacts of gas impurities on the minimum miscibility pressure of injected CO2-rich gas–crude oil systems and enhanced oil recovery potential. *Pet. Sci.* **16**, 117–126 (2018).

(42) Yang, K. *et al.* Research on component variation and factors affecting minimum miscible pressure in low viscosity oil miscibility process. *ACS Omega* **9**, 30131–30141 (2024).

(43) Yang, Z. *et al.* Reducing the minimum miscibility pressure of CO2 and crude oil using alcohols. *Colloids Surf. Physicochem. Eng. Asp.* **568**, 105–112 (2019).

(44) Liu, J., Sun, L., Li, Z. & Wu, X. Experimental Study on Reducing CO2–Oil Minimum Miscibility Pressure with Hydrocarbon Agents. *Energies* **12**, (2019).

(45) Zhang, C., Xi, L., Wu, P. & Li, Z. A novel system for reducing CO2-crude oil minimum miscibility pressure with CO2-soluble surfactants. *Fuel* **281**, 118690 (2020).

(46) Zhao, Y. *et al.* The experimental research for reducing the minimum miscibility pressure of carbon dioxide miscible flooding. *Renew. Sustain. Energy Rev.* **145**, 111091 (2021).

(47) Wang, X., Zhang, S. & Gu, Y. Four Important Onset Pressures for Mutual Interactions between Each of Three Crude Oils and CO_2. *J. Chem. Eng. Data* **55**, 4390–4398 (2010).

(48) Zhang, K. & Gu, Y. Two new quantitative technical criteria for determining the minimum miscibility pressures (MMPs) from the vanishing interfacial tension (VIT) technique. *Fuel* **184**, 136–144 (2016).

(49) Al-Hakami, M. A. *et al.* Improving CO2 Miscibility in Crude Oil Utilizing Viscosity Reducer: Experimental and Molecular Simulation Study. *Arab. J. Sci. Eng.* **50**, 21455–21467 (2025).

(50) Zhang, H., Hou, D. & Li, K. An Improved CO_2 -Crude Oil Minimum Miscibility Pressure Correlation. *J. Chem.* **2015**, 175940 (2015).

(51) Chen, H., Li, B., Duncan, I., Elkhider, M. & Liu, X. Empirical correlations for prediction of minimum miscible pressure and near-miscible pressure interval for oil and CO2 systems. *Fuel* **278**, 118272 (2020).

(52) Yellig, W. F. & Metcalfe, R. S. Determination and Prediction of CO2 Minimum Miscibility Pressures (includes associated paper 8876). *J. Pet. Technol.* **32**, 160–168 (1980).

(53) Orr, F. M. & Jensen, C. M. Interpretation of Pressure-Composition Phase Diagrams for CO2/Crude-Oil Systems. *Soc. Pet. Eng. J.* **24**, 485–497 (1984).

(54) Prakash, S. & Mandal, A. Validation of Empirical Minimum Miscibility Pressure Correlations Using the Vanishing Interfacial Tension Method: Applications in CO_2 -Enhanced Oil Recovery and Carbon Capture, Utilization, and Storage. *Energy Fuels* **39**, 23229–23240 (2025).

(55) Li, H., Qin, J. & Yang, D. An Improved CO_2 –Oil Minimum Miscibility Pressure Correlation for Live and Dead Crude Oils. *Ind. Eng. Chem. Res.* **51**, 3516–3523 (2012).

(56) Emera, M. K. & Sarma, H. K. Use of genetic algorithm to estimate CO2–oil minimum miscibility pressure—a key parameter in design of CO2 miscible flood. *J. Pet. Sci. Eng.* **46**, 37–52 (2005).

(57) Holm, L. W. & Josendal, V. A. Mechanisms of Oil Displacement By Carbon Dioxide. *J. Pet. Technol.* **26**, 1427–1438 (1974).

(58) Holtz, H., Núñez-López, V. & Breton, c. Moving Permian Basin Technology to the Gulf Coast: The Geologic Distribution of CO2 EOR Potential in Gulf Coast Reservoirs. *AAPG* https://api.semanticscholar.org/CorpusID:208332430 (2005).

(59) Alston, R. B., Kokolis, G. P. & James, C. F. CO2 Minimum Miscibility Pressure: A Correlation for Impure CO2 Streams and Live Oil Systems. *Soc. Pet. Eng. J.* **25**, 268–274 (1985).